CHEMISTRY OF MATERIALS

Article

pubs.acs.org/cm

Photophysical Properties of Near-Infrared Phosphorescent π-Extended Platinum Porphyrins

Jonathan R. Sommer, Abigail H. Shelton, Anand Parthasarathy, Ion Ghiviriga, John R. Reynolds, and Kirk S. Schanze*

Department of Chemistry and Center for Macromolecular Science and Engineering, University of Florida, Gainesville, Florida 32611-7200, United States

Supporting Information

ABSTRACT: A comprehensive photophysical study is reported on a family of π-extended platinum(II) porphyrin complexes. The platinum(II) complexes are synthesized from the corresponding free base porphyrins by treatment with platinum(II) acetate in hot benzonitrile, affording the complexes in considerably higher yield than by reaction with platinum(II) chloride. A quantitative study of the absorption and luminescence properties of the metalloporphyrins is presented. A series including tetraarylbenzo-, tetraarylnaphtho-, and tetraarylanthroporphyrin exhibits efficient phosphorescence at 773, 890, and 1020 nm in the near-infrared region, with quantum yields of 0.35, 0.15, and 0.08, respectively. The triplet lifetimes and phosphorescence yields decrease with increasing emission wavelength, consistent with energy gap law behavior. A set of six Pt-tetrabenzoporphyrins (TBPs) with different meso-substituents were examined. The Pt-TBPs exhibit efficient phosphorescence with $\lambda_{max} \sim 770$ nm and with a quantum yield ranging from 0.26−0.49, depending on the substitution pattern. The results show that the 5,15-diarylbenzoporphyrins feature 50−60% higher phosphorescence emission yield compared to the 5,10,15,20-tetraarylbenzoporphyrins. The highest phosphorescence quantum efficiency is observed for a platinum(II) 5,15-diarylbenzoporphyin which emits at 770 nm with a quantum yield of 49%.

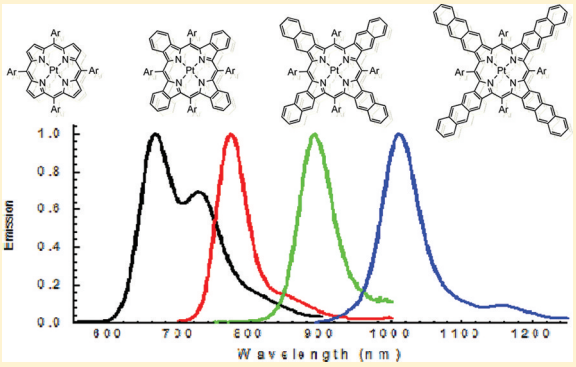

KEYWORDS: *platinum porphyrin, benzoporphyrin, π-conjugated, near-infrared, phosphorescence*

INTRODUCTION

Porphyrins with aromatic rings fused to the β-positions of the pyrrole residues are referred to as π-extended porphyrins, and they have attracted significant attention in recent years as optoelectronic materials.[1−5] The increased conjugation afforded by the fused rings to the porphyrin macrocycle leads to enhanced light absorption and efficient emission in the near-infrared (near-IR) region of the spectrum. In particular, the optical properties of these materials in the near-IR draw interest for use in numerous applications ranging from biomedical sensing and imaging to electrooptics.[2−6] Consequently π-extended porphyrins have been desired synthetic targets dating back to when initial work on the effects of π-extension on the optical properties of porphyrins was carried out in the 1960s.[7−9] Until recently, applications of π-extended porphyrins were hindered because of the difficulty of synthesizing the free-base porphyrins in sufficient yields. However, the large potential of these materials in a broad range of applications has fueled recent progress toward synthesis of the free-base porphyrins, along with a few metal complexes.[10−14] The photophysical properties of some π-extended porphyrins have also been reported,[2,3,14−20] although much work still remains for this interesting class of molecular chromophores.

One area of growing interest concerns the synthesis and properties of platinum(II) complexes of π-extended porphyrins. In general, platinum(II) porphyrins have proven to be important chromophores for a variety of applications, mainly because of their propensity to exhibit high quantum yield and long-lived phosphorescence. Thus, documenting the properties of platinum(II) complexes of π-extended porphyrins is important, as these chromophores are expected to feature large absorptivity in the near-IR region, and exhibit high quantum efficiency near-IR phosphorescence. Indeed, recent work by Thompson and co-workers demonstrates that a platinum(II) tetrabenzoporphyrin (TBP) complex features efficient near-IR phosphorescence at ∼770 nm, and it has been used as a phosphor in highly efficient near-IR emitting organic light emitting diodes.[16] Moreover, we recently reported light emitting diodes based on a platinum(II) tetranaphthoporphyrin that emit at ∼900 nm.[21]

Herein, we report a detailed investigation that characterizes the photophysical properties of the family of platinum(II) π-extended porphyrins shown in Figure 1. The study is broken

Received: August 1, 2011
Revised: November 2, 2011
Published: November 3, 2011

dx.doi.org/10.1021/cm202241e | *Chem. Mater.* 2011, 23, 5296−5304

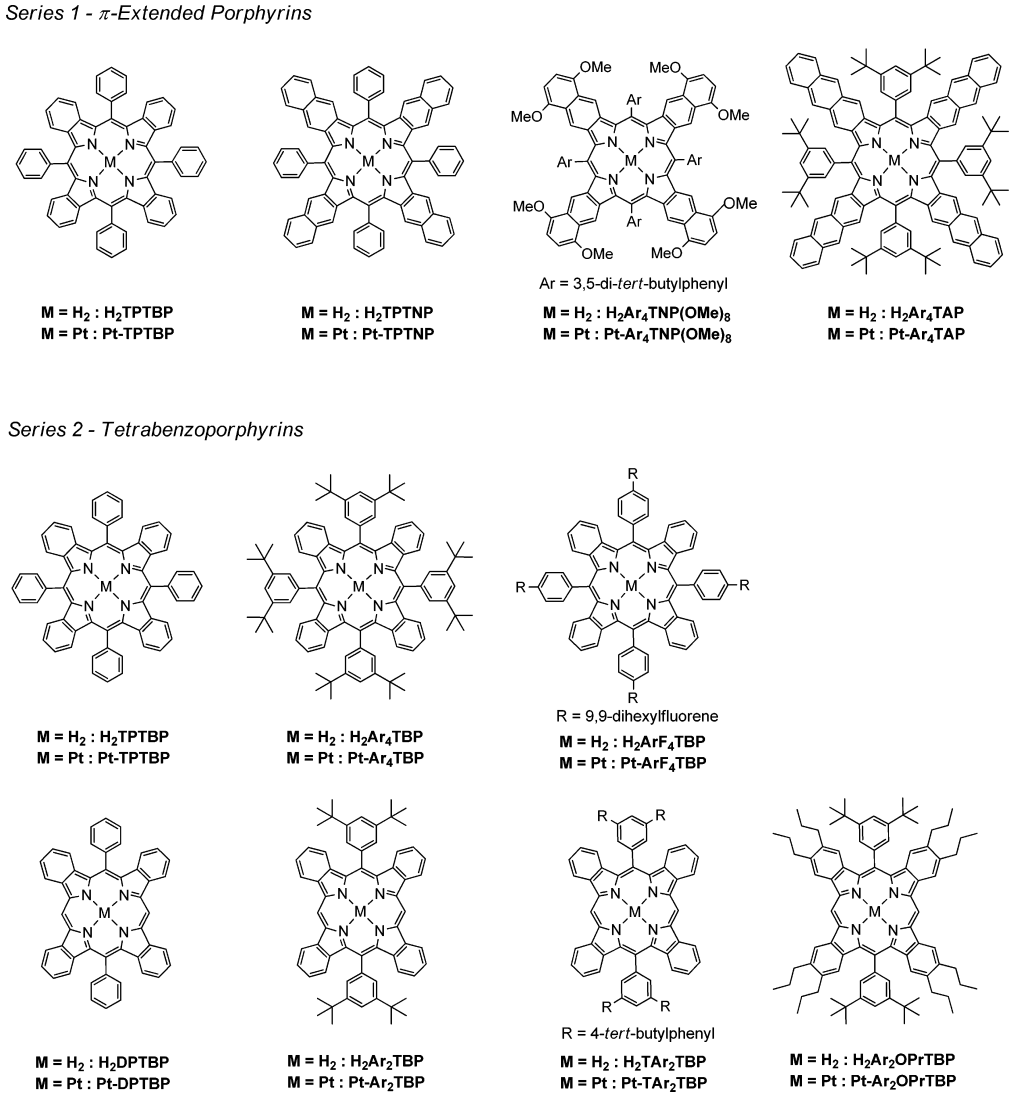

Figure 1. Structures of free-base and platinum π-extended porphyrins.

down into two sets of chromophores. In the first set (Series-1) we explore the effects of extending the π-conjugation on the phosphorescence energy, lifetime, and quantum yield of the porphyrin chromophores. An energy gap law effect is observed across this series, which gives rise to a decrease in the emission quantum yield with decreasing phosphorescence energy. In the second set (Series 2) we explore the effect of meso-substitution on a family of platinum(II) tetrabenzoporphyrins. Each of the TBP complexes exhibits intense phosphorescence at ∼770 nm, and the quantum yield and lifetime of the emission increase substantially for the 5,15-disubstituted chromophores relative to those with 5,10,15,20-tetraryl substitution. Although there have been a number of previous studies of free-base and metallo-substituted π-extended porphyrins,[1,3,15,16,21] this is the first comprehensive report which compares the properties of a broad family of platinum(II) complexes. A companion paper describes the application of this series of Pt(II) expanded conjugation porphyrins in organic- and polymer light emitting diodes.[22]

RESULTS AND DISCUSSION

Structures and Synthesis. The structures of the free-base and platinum(II) complexes of π-extended porphyrins studied in this work are shown in Figure 1 (see Supporting Information for details on the synthesis of the starting materials and the free-base porphyrins). The free-base porphyrins were prepared via the recently developed dihydroisoindole method.[2,14,23,24] To date only 4 of the 10 free-base porphyrins in Figure 1 have been previously reported (H_2TPTBP, H_2DPTBP, H_2Ar_2TBP, and H_2TPTNP).[14,23,24] While derivatives and some metal complexes have been reported for two of the other free-base porphyrins (i.e., $H_2Ar_4TNP(OMe)_8$ and H_2Ar_4TAP), there has not been a previous study which has systematically explored the relationship between structure and photophysical properties for this important family of molecular chromophores.[14,18] In particular, most of the known photophysical data for the free-base π-extended porphyrins in Figure 1 is focused on the tetrabenzoporphyrin derivatives.[17,23,24] Metalloporphyrins have been reported for specific examples from both Series 1 and 2 in Figure 1, with Zn(II) and Pd(II) complexes being the best explored systems.[2,14,17,18] A few literature reports have also described a limited set of photophysical data for free-base and metallo-tetrabenzoporphyrins and tetranaphthoporphyrins.[15,17] However, to date platinum(II) complexes of π-extended porphyrins have only been reported for a few tetrabenzoporphyrin derivatives.[1,3,15,16]

dx.doi.org/10.1021/cm202241e | Chem. Mater. 2011, 23, 5296–5304

The classical approach used to prepare Pt(II) porphyrins involves reacting the free base porphyrin with excess (molar equivalents) $PtCl_2$ in refluxing benzonitrile (>190 °C). It is believed that benzonitrile and $PtCl_2$ react to form a Pt(II)-benzonitrile complex that enhances the solubility of the platinum reagent in the reaction medium. However, despite the increase in solubility, metalation often proceeds slowly; therefore, long reaction times are often required (24 h is typical). Complexation of the metal to the porphyrin center increases the symmetry of the porphyrin chromophore, leading to significant shifts in the predominant absorption bands (Soret and Q-bands). Therefore, the metalation reaction is often followed by UV−visible absorption spectroscopy; specifically, the reaction progress is monitored by the changes in the Soret and Q-bands characteristic of the free-base porphyrin reactant and the metalloporphyrin product.

Thompson and co-workers recently reported preparation of Pt-TPTBP via reaction of a free-base tetrahydrobenzoporphyrin precursor with $PtCl_2$ in refluxing benzonitrile followed by oxidation of the metalated porphyrin with DDQ to form the TBP ring.[16] This overall two-step process afforded Pt-TPTBP in a relatively low yield (30%). In the course of the present investigation, the initial reaction used to prepare Pt-TPTNP (Scheme 1) by reacting H_2TPTNP with $PtCl_2$ in hot benzonitrile (200 °C) was monitored by UV−visible absorption spectroscopy (Supporting Information, Figure S-1). The reaction was followed for 5 h, and, during this period, the metalated Pt-TPTNP was not observed in the absorption spectrum. A small amount of Pt-TPTNP could be detected in the UV−visible absorption spectrum after the reaction mixture was heated to higher temperature (>230 °C); however, these conditions are impractical because of decomposition of H_2TPTNP.

Scheme 1. Synthetic Scheme for π-Extended Pt(II) Porphyrins

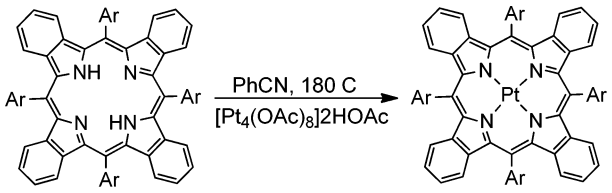

Pt-TPTBP (74%) **Pt-TAr$_2$TBP** (55%)
Pt-Ar$_4$TBP (35%) **Pt-Ar$_2$OPrTBP** (58%)
Pt-ArF$_4$TBP (94%) **Pt-TPTNP** (53%)
Pt-DPTBP (25%) **Pt-Ar$_4$TNP(OMe)$_8$** (85%)
Pt-Ar$_2$TBP (32%) **Pt-Ar$_4$TAP** (38%)

A careful literature survey suggested that metal(II) acetate complexes may undergo reaction under milder conditions with free base porphyrins;[25] thus, we decided to attempt to use platinum(II) acetate as a reagent to metalate the expanded conjugation porphyrins. Platinum(II) acetate is currently not commercially available, but it is readily prepared by reacting $PtCl_2$ with silver acetate in refluxing acetic acid under an inert atmosphere.[26] Platinum(II) acetate provides two main advantages over other platinum(II) reagents with respect to porphyrin metalation in that it is highly soluble in good solvents for porphyrins (CH_2Cl_2 and $CHCl_3$), and it has a higher reactivity compared to the halogen salts. UV−visible absorption spectroscopy shows that reaction of platinum(II) acetate with H_2TPTNP in benzonitrile (180 °C) leads to rapid formation of Pt-TPTNP (<30 min reaction time, Supporting Information, Figure S-1). After approximately 5 h the absorption spectrum reveals that the reaction is essentially complete; the Soret and Q-bands of H_2TPTNP have completely disappeared in favor of the absorptions of the metalated product. This reaction affords a method for preparation of π-extended platinum(II) porphyrins at lower temperatures using shorter reaction times, resulting in improved yields compared to the traditional route based on $PtCl_2$. Metalation with platinum(II) acetate has allowed us to prepare platinum-(II) complexes of the tetranaphthoporphyrin and tetraanthryl-porphyrin chromophores for the first time, while also providing improved yields in the synthesis of previously reported platinum tetrabenzoporphyrins. In this work the target π-extended platinum(II) porphyrin complexes (Figure 1) were all prepared by reacting the free-base with platinum(II) acetate in a manner similar to that used to prepare Pt-TPTNP (Scheme 1). The materials were subjected to vacuum distillation to remove the high boiling solvent followed by chromatography and multiple precipitations to remove trace amounts of free-base starting material prior to characterization by ^{1}H and ^{13}C NMR and HRMS.

Photophysics of Free-Base π-Extended Porphyrins (Series 1). Initially, we describe the effect of increased π-conjugation on the photophysical properties of the free-base benzoporphyrins in Series 1; then we will turn to the platinum(II) complexes. The absorption and fluorescence spectra obtained in toluene solution for the Series 1 free-base porphyrins are shown in Figure 2, and Table 1 collects pertinent data including the absorption and fluorescence wavelength maxima, the absorption coefficients, fluorescence quantum yields (ϕ_{fl}), and fluorescence lifetimes (τ_{fl}).

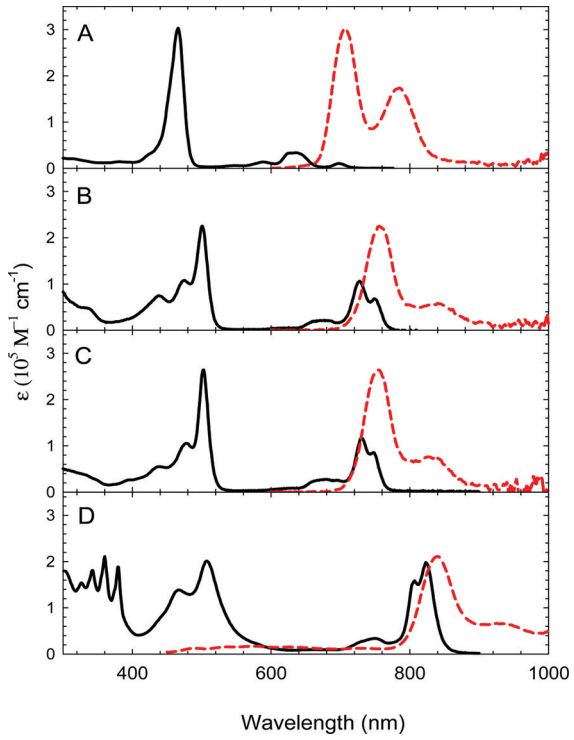

Figure 2. Absorption (black solid lines) and fluorescence (red dashed lines) of Series 1 free-base π-extended porphyrins in air saturated toluene. (A) H_2TPTBP, (B) H_2TPTNP, (C) $H_2Ar_4TNP(OMe)_8$, and (D) H_2Ar_4TAP.

dx.doi.org/10.1021/cm202241e | Chem. Mater. 2011, 23, 5296−5304

Table 1. Photophysical Properties of Series 1 Free-Base π-Extended Porphyrins[a]

free-base porphyrins	absorption λ_{max} / nm Soret, Q-band (log ε_{max}/M^{-1} cm^{-1})	fluorescence λ_{max} / nm	ϕ_{fl} (τ_{fl} / ns)	k_r / s^{-1} (k_{nr} / s^{-1})
H_2TPTBP	465 (5.48)	704, 785	0.031 ± 0.01	9.9×10^6
	633 (4.52)		(3.1)	(3.1×10^8)
H_2TPTNP	500 (5.35)	756, 840	0.14 ± 0.02	3.7×10^7
	728 (5.02)		(3.9)	(2.2×10^8)
$H_2Ar_4TNP(OMe)_8$	502 (5.42)	755, 837	0.17 ± 0.01	3.8×10^7
	730 (5.07)		(4.6)	(1.8×10^8)
H_2Ar_4TAP	510 (5.32)	841, 932	0.051 ± 0.05	5.1×10^7
	824 (5.29)		(1.0)	(9.5×10^8)

[a]Measured in air-saturated toluene solutions. Fluorescence quantum yields were measured relative to ZnTPP in toluene (ϕ_{fl} = 0.03).[27−29] Fluorescence decays obtained by time-correlated single photon counting, and the decays followed single exponential kinetics.

The addition of fused-aromatic rings to the pyrrole units of the porphyrin macrocycle across the series from H_2TPTBP to H_2Ar_4TAP gives rise to an approximately 200 nm red shift of the Q-band absorption. This results in the transition shifting from the red region of the visible (H_2TPTBP) fully into the near-IR region of the spectrum (H_2Ar_4TAP). The Q-band oscillator strength increases substantially across the series as evidenced by the nearly 10-fold increase in molar absorptivity constant from H_2TPTBP to H_2Ar_4TAP ($\varepsilon = 3.32 \times 10^4 - 1.95 \times 10^5$ M^{-1} cm^{-1}). However the Soret band is only red-shifted 50 nm across the series from H_2TPTBP to H_2Ar_4TAP. The Soret transition is strongly allowed and remains in the midvisible region ($\varepsilon \sim (2-3) \times 10^5$ M^{-1} cm^{-1}). Interestingly, the absorption of anthroporphyrin H_2Ar_4TAP features a transition in the near-UV region (340−400 nm) which exhibits a well-defined vibronic progression. This transition is similar to that of the lowest energy absorption of anthracene, and it is thus likely that in H_2Ar_4TAP the absorption feature arises from transitions localized on the fused anthryl units.

The photoluminescence of the Series 1 free-base porphyrins appears as a single fluorescence band (split into vibronic subbands) that exhibits a small Stokes shift relative to the lowest energy Q-band (Figure 2). Across the series H_2TPTBP to H_2Ar_4TAP the fluorescence maxima red-shift by approximately 140 nm. The quantum yield for H_2TPTBP in toluene (~0.03) is in good agreement with the reported literature value.[17] Interestingly, ϕ_{fl} is substantially larger for the naphthoporphyrins (H_2TPTNP and $H_2Ar_4TNP(OMe)_8$). This trend results from a significant increase in the radiative decay rate constant (k_r, Table 1); the increased radiative decay rate is consistent with the increase in the "allowedness" of the S_1-S_o transition induced by the π-extended arylene ring systems.

Ono et al. have reported the fluorescence spectra for two fluorescent zinc(II) tetraanthroporphyrins; however, photophysical characterization of a free-base tetraanthroporphyrin has not been reported previously.[18] The fluorescence of H_2Ar_4TAP is dominated by a band with λ_{max} = 841 nm with a vibronic shoulder at 932 nm. Interestingly, this compound exhibits broad, weak fluorescence throughout the visible region; this emission is believed to arise from S_n-S_o radiative decay arising from the porphyrin ring- and anthryl-based chromophores. Despite having a larger radiative decay rate, the fluorescence yield for H_2Ar_4TAP (0.051) is significantly less than that for the tetranaphthoporphyins. This anomaly arises because the nonradiative decay (k_{nr}) rate is substantially larger for the anthroporphyrin. Nonetheless, the fluorescence quantum yield for H_2Ar_4TAP is sufficiently large to make this system a notable near-IR fluorescent chromophore.

Photophysics of Platinum(II) π-Extended Porphyrins (Series-1). The photoluminescence spectra from Series 1 π-extended platinum porphyrins are shown in Figure 3, and photophysical parameters are summarized in Table 2. The emission spectra are dominated by a single phosphorescence band with a weak vibronic shoulder. No fluorescence is seen in the spectra, indicating that the rate of singlet−triplet intersystem crossing is rapid, as promoted by the strong spin−orbit coupling imparted by platinum. In addition, the efficient phosphorescence seen for all of the Series 1 platinum(II) complexes (Table 2) is also the result of the strong platinum induced spin−orbit coupling which promotes radiative decay from the lowest triplet state (T_1). For each of these complexes, the phosphorescence band is shifted significantly to the red from the lowest Q-band absorption. The singlet−triplet splitting value (E_{ST}, Table 2) for each complex was computed based on the energy difference between the fluorescence (of the free-base) and the phosphorescence, and the splitting is relatively constant at ~0.3 eV across the

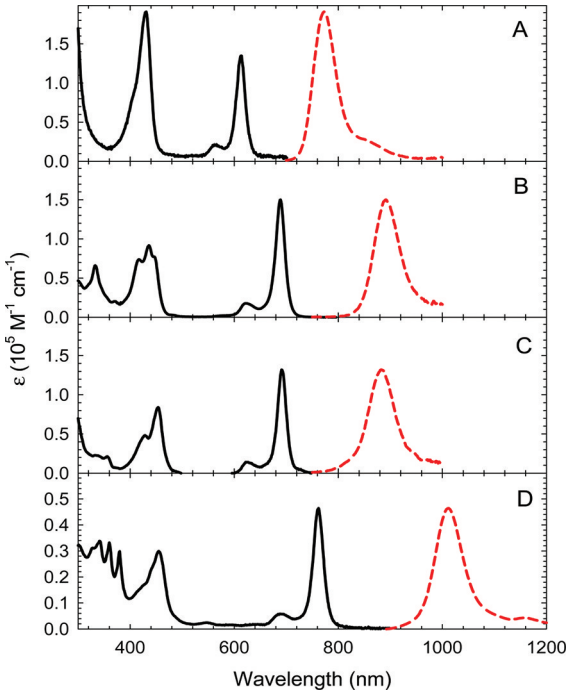

Figure 3. Absorption (black solid lines) and phosphorescence (red dashed lines) of Series 1 π-extended platinum porphyrins in toluene. (A) Pt-TPTBP, (B) Pt-TPTNP, (C) Pt-$Ar_4TNP(OMe)_8$, and (D) Pt-Ar_4TAP (Note *Y*-axis scale is different).

dx.doi.org/10.1021/cm202241e | *Chem. Mater.* 2011, 23, 5296−5304

Table 2. Photophysical Data for Series 1 π-Extended Platinum(II) Porphyrins[a]

platinum porphyrins	absorption λ_{max} / nm Soret, Q-band (log ε_{max}/M^{-1} cm^{-1})	emission λ_{max} / nm	ϕ_p[b] (τ_T / μs)[c]	k_r / s^{-1} (k_{nr} / s^{-1})	E_{ST} / eV
Pt-TPTBP	430 (5.28)	773	0.35 ± 0.05	1.2×10^4	0.33
	612 (5.13)		(29.9)	(2.2×10^4)	
Pt-TPTNP	436 (4.96)	891	0.15 ± 0.001	1.2×10^4	0.34
	689 (5.17)		(12.7)	(6.7×10^4)	
Pt-Ar$_4$TNP(OMe)$_8$	455 (4.92)	883	0.12 ± 0.005	7.8×10^3	0.32
	690 (5.12)		(15.3)	(5.8×10^4)	
Pt-Ar$_4$TAP	455 (4.47)	1022	0.08 ± 0.02	2.6×10^4	0.35
	762 (4.66)		(3.2)	(2.9×10^5)	

[a]Measured in vacuum degassed toluene solutions. [b]Emission quantum yields measured relative to ZnTPP (ϕ_{fl} = 0.03),[27−29] with the exception of Pt-Ar$_4$TAP which was measured relative to H$_2$TPTBP (ϕ_{fl} = 0.031) with excitation at 420 nm. [c]Triplet lifetimes (τ_T) were determined by transient absorption spectroscopy.

series. Importantly, the phosphorescence emission for all of the Series 1 porphyrins is well into the near-IR region, ranging from ∼773 nm for the benzoporphyrin to ∼1020 nm for the anthroporphyrin, making these complexes significant from the standpoint of near-IR phosphor applications.

Phosphorescence quantum yields (ϕ_p) were measured for the Series 1 Pt-porphyrins, and the values are listed in Table 2. The phosphorescence yields are comparatively large, ranging from 0.35 for Pt-TPTBP to 0.08 for Pt-Ar$_4$TAP. The triplet lifetimes (τ_T) were determined by transient absorption spectroscopy, and the values range from ∼30 μs for Pt-TPTBP to 3.2 μs for Pt-Ar$_4$TAP. (The triplet−triplet absorption spectra are included in the Supporting Information, Figure S-4). Interestingly, it is evident that τ_T systematically decreases with phosphorescence energy, suggesting that the emission decay of this series follows an energy gap law dependence.[30−32] By using the ϕ_p and τ_T values we have computed the radiative and nonradiative decay rates for the triplet states (k_r and k_{nr}, respectively, Table 2). Here, it is seen that the radiative rates are relatively constant across the series; however, the nonradiative decay rate clearly increases as the emission energy decreases. An analysis of the energy gap law dependence of the triplet decay rates is shown in Supporting Information, Figure S-7 (plot of ln(k_{nr}) vs E_{em}), and it is clear from this correlation that the triplet lifetime (and consequently the phosphorescence yield) for this family of phosphors is ultimately limited by the triplet-ground state energy gap.[30−32]

Comparison of our results with previous work in the literature reveals some interesting and useful points. First, the phosphorescence quantum yield and triplet lifetime values for Pt-TPTBP reported by Thompson et al. (53 μs, 0.70) differ from our measurements (29.9 μs, 0.35), but our results are in line with those reported for the same complex by Kilmant et al.[3,16] We note that the quantum yield reported by Thompson was based on an extrapolation from a low temperature measurement where it was assumed that the quantum yield was unity. Second, on the basis of a literature report for a palladium(II) octamethoxy substituted tetranaphthoporphrin,[14] we expected that the phosphorescence for Pt-Ar$_4$TNP(OMe)$_8$ might be red-shifted relative to Pt-TPTNP. However, it is evident that these two complexes exhibit virtually identical photophysical behavior, perhaps not surprisingly as the methoxy groups are not expected to interact strongly with the porphyrin chromophore.

Photophysics of Platinum(II) Benzoporphyrins (Series 2). To explore the effect of ring substitution on the photophysics of platinum(II) π-extended conjugation porphyrins we examined the Series 2 Pt(II)-benzoporphyrin complexes (Figure 1). This series was designed to examine the effect of *meso* substitution as well as the use of bulky substitutents on the benzoporphyrin periphery to enhance solubility and minimize the tendency of the macrocycle to aggregate. The latter effect may be especially important in organic- and polymer-LED application where the porphyrin chromophores are present at high concentration in the solid state.[33,34] The ultimate goal of this work was to optimize the phosphorescence yield for the Pt(II)-benzoporphyrin system, which would then advance this system for use in high efficiency near-IR OLED and PLED application.

Our work on the Series 2 benzoporphyrins was inspired by a recent report by Vinogradov and co-workers which systematically examined the relationship between porphyrin substitution and photophysics for a series of free-base and Pd(II)-benzoporphyrins.[17] Especially pertinent to the present study was their observation that the lifetime and phosphorescence quantum yield for 5,15-diphenyl *meso*-substituted porphyrins Pd-DPTBP is nearly double that for corresponding 5,10,15,20-tetraphenyl substituted complex, Pd-TPTBP (0.15 vs 0.08). The lower emission yield for the tetraphenyl derivative arises because this porphyrin is more distorted from planarity (saddled conformation) because of steric interactions induced by the *meso* substituents. The decrease in planarity increases the nonradiative decay rate, shortening the triplet lifetime and phosphorescence yield.[17] Other reports have also shown that bulky substituents that either block *meso*-aryl rotation or prevent aggregation in solution lead to an increase in the emission quantum efficiency,[33,34] and this work was considered specifically as we developed structures Pt-ArF$_4$TBP and Pt-TAr$_2$TBP which contain fluorene or *t*-butylphenyl substituents on the *meso*-phenyl groups.

The photophysical properties for the Series 2 free-base benzoporphyrins are identical to the literature reports, and our data is summarized in the Supporting Information.[17] The absorption and photoluminescence obtained in deoxygenated toluene solutions for selected Series 2 platinum benzoporphyrins are shown in Figure 4, while photophysical data for the entire Series 2 of platinum complexes is listed in Table 3. In each case, the absorption spectra for the Series 2 platinum benzoporphyrins are blue-shifted relative to the free-base macrocycles, consistent with porphyrins having local D_{4h} symmetry (metal center).

Comparison of the absorption spectral data in Table 3 and Figure 4 reveals that the tetraryl- and diaryl- complexes show slightly different properties. In particular, comparison of Figures 4a and 4b (Pt-Ar$_4$TBP and Pt-ArF$_4$TBP) with Figures 4c and 4d (Pt-TAr$_2$TBP and Pt-Ar$_2$OPrTBP) reveals

dx.doi.org/10.1021/cm202241e | Chem. Mater. 2011, 23, 5296−5304

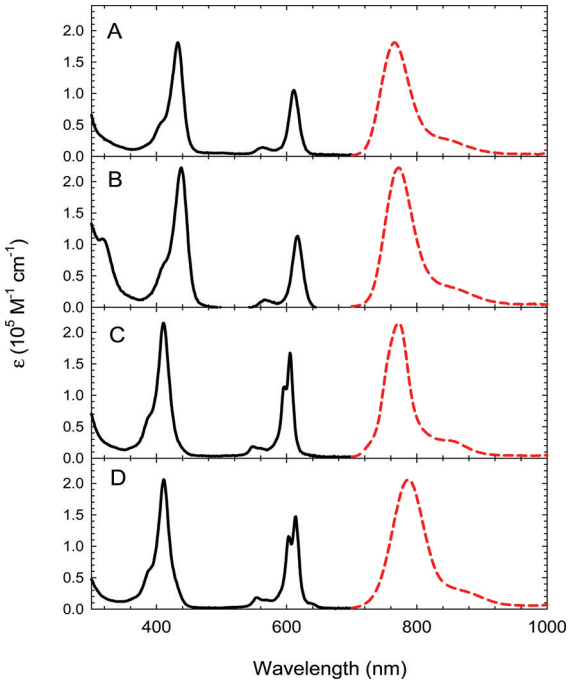

Figure 4. Absorption (black) and photoluminescence (red) of select Series 2 π-extended platinum porphyrins in deoxygenated toluene. (A) Pt-Ar_4TBP, (B) Pt-ArF_4TBP, (C) Pt-TAr_2TBP, (D) Pt-Ar_2OPrTBP.

that the Soret and Q-bands are blue-shifted for the diaryl-systems. This trend was reported previously for a series of Pd-tetrabenzoporphyrins.[17] More interestingly, the Q-band for the diaryl-porphyrins (Figure 4c and 4d) is split, likely because of the decreased symmetry of the macrocycle systems.

Comparison of the photoluminescence data in Table 3 and Figure 4 shows that all of the Pt-benzoporphyrins exhibit strong room temperature phosphorescence. In general the phosphorescence of the diaryl- complexes is slightly blue-shifted relative to that of the tetraaryl- derivatives (~770 vs 772 nm), with the exception of Pt-Ar_2OPrTBP which exhibits a distinct red-shifted phosphorescence band at 786 nm. The triplet lifetimes for the entire set of Series 2 complexes were measured by transient absorption spectroscopy, and the values are listed in Table 3, along with the phosphorescence quantum yields. These results show that the phosphorescence yields are 50−60% larger for the diaryl benzoporphyrins (Pt-Ar_2TBP, Pt-TAr_2TBP, and Pt-Ar_2OPrTBP) relative to the tetraaryl complexes (Pt-TPTBP, Pt-Ar_4TBP, Pt-ArF_4TBP). The exception to this trend is Pt-DPTBP, which exhibits a phosphorescence yield similar to that of the tetraaryl complexes. The highest quantum yield is observed for the diaryl complex Pt-Ar_2TBP with a value of 0.49. Examination of the triplet lifetimes for the series shows that there is good correlation between the phosphorescence yields and the triplet lifetimes. The diaryl substituted complexes, which exhibit more efficient phosphorescence, have lifetimes in the range of ~50 μs, whereas the tetraaryl complexes have lifetimes ~30 μs. This correlation indicates that the triplet decay rate (and consequently the phosphorescence quantum yield) is determined by the nonradiative decay rate (k_{nr}). This fact is underscored by the significant variation in k_{nr} across the series, while the radiative rate (k_r) is relatively constant at $\sim 1.0 \times 10^4$ s^{-1}.

The anomalously low phosphorescence yield and lifetime for the parent diaryl complex Pt-DPTBP may be due to the fact that rotation of the *meso*-phenyl substituents enhances the rate of nonradiative decay.[34,35] This mode of nonradiative decay is blocked by the bulky substituents in the other diaryl porphyrins, affording them with considerably higher triplet lifetimes and phosphorescence yields.

Taken together, the results on the Series 1 Pt-benzoporphyrins show that all of these chromophores exhibit efficient, relatively long-lived phosphorescence in the near-infrared region near 770 nm. As seen in previous studies, the diaryl substitution pattern gives rise to chromophores with substantially higher phosphorescence yield and lifetime compared to cogeners with tetraaryl substitution. The most efficient phosphor of the set is Pt-Ar_2TBP which exhibits a phosphorescence quantum yield of ~49%. This is believed to be the highest phosphorescence efficiency observed to date for phosphorescence from a near-infrared emitting phosphor.

SUMMARY AND CONCLUSIONS

This report describes a complete investigation of the photophysical properties of a series of expanded π-conjugation platinum(II) porphyrin chromophores that exhibit efficient phosphorescence in the near-infrared region. The series of free-base porphyrins were prepared by using techniques developed over the past several years, and metalation with platinum(II)

Table 3. Photophysical Data for Series 2 Platinum TBPs in Deoxygenated Toluene

complex	absorption λ_{max} / nm Soret, Q-band (log ε_{max} / M^{-1} cm^{-1})	emission λ_{max} / nm	$\phi_p{}^a$ (τ_T/ μs)^b	k_r / s^{-1} (k_{nr} / s^{-1})
Pt-TPTBP	430 (5.28)	773	0.35 ± 0.05	1.2×10^4
	612 (5.13)		(29.9)	(2.2×10^4)
Pt-Ar_4TBP	432 (5.26)	772	0.33 ± 0.003	1.0×10^4
	610 (5.02)		(32.0)	(2.1×10^4)
Pt-ArF_4TBP	438 (5.35)	772	0.26 ± 0.01	1.3×10^4
	617 (5.05)		(20.1)	(3.7×10^4)
Pt-DPTBP	409 (4.43)	770	0.3 ± 0.02	1.1×10^4
	604 (4.33)		(28.0)	(2.5×10^4)
Pt-Ar_2TBP	410 (5.24)	770	0.49 ± 0.08	9.2×10^3
	604 (5.12)		(53.0)	(9.7×10^3)
Pt-TAr_2TBP	411 (5.33)	769	0.44 ± 0.03	8.4×10^3
	605 (5.22)		(51.7)	(1.1×10^4)
Pt-Ar_2OPrTBP	411 (5.31)	786	0.45 ± 0.01	8.7×10^3
	614 (5.17)		(51.8)	(1.1×10^4)

[a]Phosphorescence quantum yields were measured relative to ZnTPP (0.03)[27−29] by excitation at 420 nm in toluene. [b]Triplet lifetimes were obtained by transient absorption spectroscopy.

dx.doi.org/10.1021/cm202241e | *Chem. Mater.* 2011, 23, 5296−5304

acetate afforded the metallo-pophyrins in moderate to high yield. Comparison of the photophysical properties of the expanded conjugation series reveals that the tetrabenzo-, tetranaphtho-, and tetraanthroporphyrins exhibit phosphorescence at wavelengths ranging from ~770−1020 nm. Analysis of the quantum yield and lifetime data shows that the radiative decay rates from the triplet states are relatively constant across the series; however, the nonradiative decay rate increases substantially with decreasing T_1-S_o energy gap. An energy gap law correlation is observed, which indicates there is a limited prospect for extending the emission wavelength to longer wavelengths because the phosphorescence yield will become very low. A study of an extensive set of variously substituted platinum(II) benzoporphyrins was also completed, and the results show that the 5,15-diaryl-substituted chromophores exhibit 50−60% longer triplet lifetimes and substantially enhanced phosphorescence yields compared to the 5,10,15,20 tetraryl-substitued chromophores. All of the complexes studied give rise to sufficiently efficient phosphorescence such that they show considerable promise as the phosphors for application in efficient near-infrared organic- and polymer-light emitting diodes. These applications are explored thoroughly in the accompanying paper.[22]

EXPERIMENTAL SECTION

Optical Characterization. Absorption spectra for all free-base and platinum π-extended porphyrins were measured using a PerkinElmer Lambda 25 UV−vis spectrometer. The emission spectra were obtained by excitation at the Soret band absorption maximum for each compound. Emission spectra over the range 500−1000 nm were recorded on a home-built spectrometer consisting of a 75 W Xe source, an ISA H-20 excitation monochromator, and an ISA Spex Triax 180 emission spectrometer coupled to a Spectrum-1 liquid nitrogen-cooled silicon charge coupled device detector. The emission spectra for Pt-Ar_4TAP were measured on a PTI fluorimeter equipped with InGaAs near-IR detector, or a Spex Fluorolog II equipped with InGaAs near-IR detector. All emission spectra were corrected for the spectrometer response by using correction factors generated with a primary standard lamp. The emission fluorescence and phosphorescence quantum yields were calculated relative to ZnTPP in toluene (ϕ = 0.03)[27−29] unless otherwise noted according to a previously described method.[36] The sample and actinometer solutions had matched optical density at a shared excitation wavelength. Time-resolved transient absorption spectra for π-extended platinum porphyrins in toluene were collected by using previously described laser systems for the visible and near-IR regions.[37]

Synthesis and Spectral Characterization of Platinum(II) Porphyrins. A complete description of the synthesis of all free-base porphyrins, including starting compounds, synthetic schemes, and characterization data (including NMR spectra) is provided in the Supporting Information. In the following section we describe the metallation of the free-base porphyrins and spectral characterization of the platinum(II) complexes.

Platinum(II) Tetraphenyltetrabenzoporphyrin (Pt-TPTBP). A solution of **H_2TPTBP** (49 mg, 60.1 μmol) and platinum acetate (83 mg, 60.1 μmol) in benzonitrile (25 mL) was thoroughly purged with argon. The reaction was then submerged in a preheated oil bath at 200 °C and refluxed until the Q-band of **H_2TPTBP** disappeared from the UV−vis spectrum. The solvent was removed under reduced pressure, and the crude material dissolved in DCM and filtered through a plug of Celite. The material was then loaded on silica gel and purified via column chromatography eluting with 30% CH_2Cl_2 in hexanes yielding 45 mg of the title compound (74%). ^{1}H NMR (pyridine-d_5, 500 MHz): δ = 8.35 (d, 8H), 7.96 (t, 4H), 7.92 (t, 8H), 7.42 (m, 8H), 7.37 (m, 8H); ^{13}C NMR (pyridine- d_5, 125 MHz) δ = 142.1, 138.2, 136.7, 134.2, 129.9, 129.9, 126.3, 124.8; ESI-TOF m/z 1006.2549, calcd 1006.2562.

Platinum(II) Tetra(3,5-di-*tert*-butylphenyl)tetrabenzoporphyrin (Pt-Ar_4TBP). The title compound was prepared from **H_2Ar_4TBP** (80 mg, 63.3 μmol) and platinum acetate (87 mg, 63.3 μmol) in benzonitrile (30 mL) using the procedure for **Pt-TPTBP**. The crude material was purified via column chromatography eluting with 30% CH_2Cl_2 in hexanes yielding 32 mg of the title compound (35%). ^{1}H NMR (pyridine- d_5, 500 MHz): δ = 8.31 (s, 8H), 8.17 (s, 8H), 7.51 (m, 8H), 7.44 (m, 8H), 1.46 (s, 72H); ^{13}C NMR (pyridine- d_5, 125 MHz) δ = 153.3, 138.9, 136.6, 129.0, 126.4, 125.6, 122.9, 120.5, 35.6, 32.0; DART-MS $[M+H]^+$ 1457.7687, calcd 1457.7694.

Platinum(II) Tetra(4-(9,9-dihexyl-fluorenyl)-phenyl)-tetrabenzoporphyrin (Pt-ArF_4TBP). The title compound was prepared from **H_2ArF_4TBP** (76 mg, 35.4 μmol) and platinum acetate (49 mg, 35.4 μmol) in benzonitrile (25 mL) using the procedure for **Pt-TPTBP**. The crude material was purified by chromatography eluting with 20% hexanes in CH_2Cl_2. The fractions were combined and concentrated in CH_2Cl_2 then diluted with excess MeOH to precipitate 78 mg of the title compound (94%). ^{1}H NMR (pyridine-d_5, 500 MHz): δ = 8.50 (m, 12H), 8.21 (d, 4H), 8.18 (d, 4H), 8.04 (d, 4H), 7.69 (d, 8H), 7.66 (d, 4H), 7.53 (t, 8H), 7.30 (m, 8H), 2.37 (t, 4H), 2.27 (t, 4H), 1.14 (m, 16H), 1.11 (q, 16H), 0.99 (m, 16H), 0.95 (m, 16H), 0.77 (t, 24H); ^{13}C NMR (pyridine- d_5, 125 MHz) δ = 152.9, 152.0, 142.8, 142.2, 141.7, 141.2, 140.0, 138.5, 137.2, 135.1, 128.7, 128.4, 127.9, 127.4, 126.6, 125.1, 124.0, 121.4, 121.0, 119.3, 41.0, 32.1, 30.4, 24.8, 23.2, 14.5; MALDI-TOF MS $[M+H]^+$ 2338.2735, calcd 2338.2709.

Platinum Tetraphenyltetranaphthoporphyrin (Pt-TPTNP). The title compound was prepared from **H_2TPTNP** (112 mg, 110.3 μmol) and platinum acetate (150 mg, 109.3 μmol) in benzonitrile (25 mL) using a procedure similar tor **Pt-TPTBP** with heating at 180 °C. The crude material was passed a column of neutral silica gel eluting with CH_2Cl_2:THF (9:1). The first dark green band was collected, and the solvent removed. The material was precipitated from a mixture of CH_2Cl_2 and acetonitrile. The precipitate was collected and washed repeatedly with cold MeOH yielding 70 mg of the title compound (53%). The ^{1}H and gHMBC spectrum of compound Pt-TPTNP were taken on a Varian Inova 500 NMR spectrometer, equipped with a 5 mm indirect detection probe and with z-axis gradients, and operating at 500 MHz for ^{1}H and 125 MHz for ^{13}C. The chemical shifts were referenced to the residual solvent signals, 7.22 ppm in ^{1}H and 123.9 in ^{13}C. Because of the limited solubility of Pt-TPTNP in the NMR solvent, ^{13}C chemical shifts were measured by indirect detection, in a gHMBC spectrum. ^{1}H NMR (pyridine-d_5, 500 MHz) δ 8.47−8.44 (m, 8H), 8.22−8.14 (m, 4H), 8.10−8.03 (m, 8H), 7.93 (s, 8H), 7.90−7.84 (m, 8H), 7.61 (8H, overlap with solvent); ^{13}C NMR (pyridine-d_5, 125 MHz) δ 142.4, 135.9, 134.2, 131.6, 130.5, 130.0, 129.7, 126.7, 124.1, 117.9; ESI-TOF m/z 1206.3188, calcd 1206.3157.

Platinum(II) 1,4,10,13,19,22,28,31-Octamethoxy-7,16,25,34-tetrakis(3,5-di-*tert*-butylphenyl)-tetranaphthoporphyrin (Pt-Ar_4TNP(OMe)$_8$). The title compound was prepared from **H_2Ar_4TNP(OMe)$_8$** (115 mg, 67.5 μmol) and platinum acetate (92 mg, 67 μmol) in benzonitrile (30 mL) using the procedure for **Pt-TPTBP**. The crude material was passed through a column of neutral silica gel eluting with CH_2Cl_2. The first dark green band was collected, and the solvent removed. The material was precipitated from warm $CHCl_3$ and MeOH. The precipitate was collected and washed repeatedly with cold MeOH yielding 110 mg of the title compound (85%). ^{1}H NMR (pyridine-d_5, 500 MHz): δ = 8.56 (s, 8H), 8.30 (s, 8H), 8.29 (s, 4H), 6.82 (d, 8H), 3.93 (s, 24H), 1.46 (s, 72H); ^{13}C NMR (pyridine-d_5, 125 MHz) δ = 153.6, 151.1, 136.4, 127.5, 125.0, 123.5, 119.7, 119.5, 103.3, 55.8, 35.7, 32.0; MALDI-TOF MS $[M]^+$ 1896.9161, calcd 1896.9090.

Platinum(II) Tetra(3,5-di-*tert*-butylphenyl)tetraanthroporphyrin (Pt-Ar_4TAP). Because of the sensitivity with oxygen in the presence of room light for the title compound and **H_2Ar_4TAP**, all manipulations were performed under an inert atmosphere and in a flask protected from light with foil. A Schlenk flask charged with benzonitrile (6 mL), **H_2Ar_4TAP** (59 mg, 35.5 μmol), and platinum acetate (48 mg, 35.5 μmol) was degassed by three freeze pump thaw

cycles. The mixture was heated at 180 °C under a positive pressure of argon until the disappearance of the Q-band of **H_2Ar_4TAP** (approximately 3 h). The solvent was removed by vacuum distillation, and the crude was purified by passing through a short plug of neutral silica under an argon atmosphere with CH_2Cl_2. The solvent was removed under reduced pressure to give 25 mg of the title compound (38%). ^{1}H NMR (pyridine- d_5, 500 MHz): δ = 8.71 (s, 8H), 8.53 (s, 4H), 8.53 (overlap s, 8H), 8.30 (s, 8H), 8.11 (d, 8H), 7.52 (t, 8H), 1.58 (s, 72H); ^{13}C NMR (pyridine- d_5, 125 MHz) δ = 154.5, 136.6, 132.8, 130.4, 129.1, 128.7, 128.2, 126.3, 125.2, 123.4, 118.5, 35.8, 32.1; MALDI-TOF MS $[M]^+$ 1856.8951, calcd 1856.8872.

Platinum(II) 5,15-Diphenyltetrabenzoporphyrin (Pt-DPTBP). The title compound was prepared from **H_2DPTBP** (50 mg, 75.4 μmol) and platinum acetate (104 mg, 75.7 μmol) in benzonitrile (25 mL) using the procedure for **Pt-TPTBP**. The material was loaded on silica gel, eluting with CH_2Cl_2 removing the green band (**H_2DPTBP**). The solvent was changed to an increasing gradient with a THF:CH_2Cl_2 mixture (30:70). The dark blue band was collected yielding 16 mg of the title compound (25%). Analogous to the previously reported palladium complex, NMR analysis was not possible because of low solubility of **Pt-DPTBP** in common NMR solvents.[17] The material was characterized by UV−vis and mass spectrometry. UV−vis, toluene, λ_{max}: 409 nm, 547 nm, 595 nm, 604 nm; MALDI-TOF MS $[M]^+$ 852.4518, 854.1971, 855.2001, 856.2019, 857.2050, 858.2057, 859.2082, 860.2094, 861.4855, calcd 852.1919, 854.1935, 855.1960, 856.1974, 857.1999, 858.2004, 859.2026, 860.2054.

Platinum(II) 5,15-Di(3,5-di-*tert*-butylphenyl)tetrabenzoporphyrin (Pt-Ar_2TBP). The title compound was prepared from **H_2Ar_2TBP** (65 mg, 73.3 μmol) and platinum acetate (100 mg, 73.3 μmol) in benzonitrile (30 mL) using the same procedure described above for **Pt-TPTBP**. The solvent was removed, and the crude material loaded on silica gel eluting with 15% CH_2Cl_2 in hexane collecting the blue band. The material was further purified by multiple reprecipitation from boiling $CHCl_3$ and MeOH. The precipitate was collected and repeatedly washed with MeOH yielding 25 mg of the title compound (32%). ^{1}H NMR (pyridine- d_5, 500 MHz): δ = 11.55 (s, 2H), 9.80 (d, 4H), 8.35 (s, 4H), 8.31 (s, 4H), 8.08 (t, 4H), 7.78 (t, 4H), 7.54 (d, 4H); ^{13}C NMR (pyridine- d_5, 125 MHz) δ = 153.1, 141.5, 139.0, 138.2, 136.6, 136.2, 128.1, 127.7, 126.4, 122.8, 121.5, 121.0, 97.5, 35.9, 32.0; ESI-TOF [M]+ 1080.4543, calcd 1080.4481.

Platinum(II) 5,15-Di((3,5-di-*tert*-butylphenyl)-phenyl)-tetrabenzoporphyrin (Pt-TAr_2TBP). The title compound was prepared from **H_2TAr_2TBP** (110 mg, 92.3 μmol) and platinum acetate (127 mg, 92.3 μmol) in benzonitrile (25 mL) using the procedure as described for **Pt-TPTBP**. Separation with column chromatography failed because of solubility and small differences in R_f values. The title compound was purified by multiple reprecipitation from CH_2Cl_2 and MeOH to give 70 mg (55%). ^{1}H NMR (pyridine-d_5, 500 MHz): δ = 11.60 (s, 2H), 9.86 (d, 4H), 8.93 (s, 2H), 8.84 (s, 4H), 8.12 (d, 8H), 8.08 (t, 4H), 7.99 (d, 4H), 7.81 (t, 4H), 7.63 (d, 8H), 1.34 (s, 36H); ^{13}C NMR (pyridine-d_5, 125 MHz) δ = 151.8, 143.5, 139.1, 138.3, 138.2, 136.8, 130.5, 128.2, 128.0, 127.8, 126.9, 126.9, 126.3, 121.8, 120.0, 35.0, 31.7; DART-MS $[M+H]^+$ 1383.5772, calcd 1383.5770.

Platinum(II) 5,15-Di(3,5-di-*tert*-butylphenyl)octapropyltetrabenzoporphyrin (Pt-Ar_2OPrTBP). The title compound was prepared from **$H_2Ar_2OPrTBP$** (33 mg, 23.2 μmol) and platinum acetate (32 mg, 23.2 μmol) in benzonitrile (20 mL) using the procedure described for **Pt-TPTBP**. After vacuum distillation to remove benzonitrile, the crude material was loaded on silica gel and eluted with a hexane:CH_2Cl_2 mixture (85:15) collecting the first blue band. The fractions were concentrated, and the material was precipitated by the addition of excess MeOH. The precipitate was collected to give 22 mg of the title compound (58%). ^{1}H NMR (pyridine- d_5, 500 MHz): δ = 11.86 (s, 2H), 9.83 (s, 4H), 8.36 (s, 2H), 8.33 (s, 4H), 7.42 (s, 4H), 3.11 (t, 8H), 2.95 (t, 8H), 1.90 (sex, 8H), 1.82 (sex, 8H), 1.63 (s, 36H), 1.18 (t, 12H), 1.12 (t, 12H); ^{13}C NMR (pyridine- d_5, 125 MHz) δ = 153.0, 140.7, 140.4, 137.6, 136.8, 127.7, 126.8, 123.5, 121.7, 120.3, 97.0, 36.4, 35.9, 32.2, 25.6, 15.0; ESI-TOF m/z 1416.8265, calcd 1416.8301.

■ ASSOCIATED CONTENT

Ⓢ Supporting Information

Complete synthesis details, and full spectroscopic characterization of all intermediates and target free-base porphyrins including, absorption, fluorescence, and photophysical data for Series 2 free base porphyrins, transient absorption spectra of all Pt-porphyrin derivatives, energy gap law plot for Series 1 Pt-porphyrins, ^{1}H and ^{13}C NMR spectra for important intermediates, free-base and Pt-porphyrins, and peak assignment for ^{1}H and ^{13}C chemical shifts for Pt-porphyrins determined by 2D NMR (1 Table, 25 figures, 9 schemes, and 28 pages of text). This material is available free of charge via the Internet at http://pubs.acs.org.

■ AUTHOR INFORMATION

Corresponding Author

*E-mail: kschanze@chem.ufl.edu. Phone: 352-392-9133.

■ ACKNOWLEDGMENTS

We gratefully acknowledge financial support from the U.S. Army Aviation and Missile Research, Development, and Engineering Center (AMRDEC) (Project No. W31P4Q-08-1-0003).[38]

■ REFERENCES

(1) Sun, Y.; Borek, C.; Hanson, K.; Djurovich, P. I.; Thompson, M. E.; Brooks, J.; Brown, J. J.; Forrest, S. R. *Appl. Phys. Lett.* **2007**, *90*, 213503.
(2) Yakutkin, V.; Aleshchenkov, S.; Chernov, S.; Miteva, T.; Nelles, G.; Cheprakov, A.; Baluschev, S. *Chem.—Eur. J.* **2008**, *14*, 9846−9850.
(3) Borisov, S. M.; Nuss, G.; Haas, W.; Saf, R.; Schmuck, M.; Kilmant, I. *J. Photochem. Photobiol. A.* **2009**, *201*, 128−135.
(4) Kumar, R.; Ohulchanskyy, T. Y.; Roy, I.; Gupta, S. K.; Borek, C.; Thompson, M. E.; Prasad, P. N. *ACS Appl. Mater. Interfaces* **2009**, *1*, 1474−1481.
(5) Perez, M. D.; Borek, C.; Djurovich, P. I.; Mayo, E. I.; Lunt, R. R.; Forrest, S. R.; Thompson, M. E. *Adv. Mater.* **2009**, *21*, 1517−1520.
(6) Singh-Rachford, T. N.; Haefele, A.; Ziessel, R.; Castellano, F. N. *J. Am. Chem. Soc.* **2008**, *130*, 16164−16165.
(7) Gouterman, M. *J. Mol. Spectrosc.* **1961**, *6*, 138−163.
(8) Bajema, L.; Gouterman, M.; Rose, C. B. *J. Mol. Spectrosc.* **1971**, *39*, 421−431.
(9) Edwards, L.; Gouterman, M.; Rose, C. B. *J. Am. Chem. Soc.* **1976**, *98*, 7638−7641.
(10) Ito, S.; Murashima, T.; Uno, H.; Ono, N. *Chem. Commun.* **1998**, 1661−1662.
(11) Ito, S.; Ochi, N.; Uno, H.; Murashima, T.; Ono, N. *Chem. Commun.* **2000**, 893−894.
(12) Finikova, O. S.; Cheprakov, A.; Beletskaya, I. P.; Vinogradov, S. A. *Chem. Commun.* **2001**, 261−262.
(13) Finikova, O. S.; Cheprakov, A. V.; Carroll, P. J.; Vinogradov, S. A. *J. Org. Chem.* **2003**, *68*, 7517−7520.
(14) Finikova, O. S.; Aleshchenkov, S. E.; Brinas, R. P.; Cheprakov, A. V.; Carroll, P. J.; Vinogradov, S. A. *J. Org. Chem.* **2005**, *70*, 4617−4628.
(15) Finikova, O. S.; Cheprakov, A.; Vinogradov, S. A. *J. Org. Chem.* **2005**, *70*, 9562−9572.
(16) Borek, C.; Hanson, K.; Djurovich, P. I.; Thompson, M. E.; Aznavour, K.; Bau, R.; Sun, Y.; Forrest, S. R.; Brooks, J.; Michalski, L.; Brown, J. *Angew. Chem., Int. Ed.* **2007**, *46*, 1109−1112.
(17) Lebedev, A. Y.; Filatov, M. A.; Cheprakov, A. V.; Vinogradov, S. A. *J. Phys. Chem. A* **2008**, *112*, 7723−7733.
(18) Yamada, H.; Kuzuhara, D.; Takahashi, T.; Shimizu, Y.; Uota, K.; Okujima, T.; Uno, H.; Ono, N. *Org. Lett.* **2008**, *10*, 2947−2950.

(19) Rogers, J. E.; Nguyen, K. A.; Hufnagle, D. C.; McLean, D. G.; Su, W. J.; Gossett, K. M.; Burke, A. R.; Vinogradov, S. A.; Pachter, R.; Fleitz, P. A. *J. Phys. Chem. A* **2003**, *107*, 11331−11339.
(20) Lebedev, A. Y.; Cheprakov, A. V.; Sakadzic, S.; Boas, D. A.; Wilson, D. F.; Vinogradov, S. A. *ACS Appl. Mater. Interfaces* **2009**, *1*, 1292−1304.
(21) Sommer, J. R.; Farley, R. T.; Graham, K. R.; Yang, Y. X.; Reynolds, J. R.; Xue, J. G.; Schanze, K. S. *ACS Appl. Mater. Interfaces* **2009**, *1*, 274−278.
(22) Graham, K. R.; Yang, Y.; Sommer, J. R.; Shelton, A. H.; Schanze, K. S.; Xue, J.; Reynolds, J. R. *Chem. Mater.*, Web ASAP, DOI: 10.1021/cm202242x.
(23) Filatov, M. A.; Cheprakov, A. V.; Beletskaya, I. P. *Eur. J. Org. Chem.* **2007**, 3468−3475.
(24) Filatov, M. A.; Lebedev, A. Y.; Vinogradov, S. A.; Cheprakov, A. V. *J. Org. Chem.* **2008**, *73*, 4175−4185.
(25) Guseva, G. B.; Antina, E. V.; V'yugin, A. I.; Mamardashvili, G. M.; Petrov, V. V. *Russ. J. Coord. Chem.* **2006**, *32*, 116−120.
(26) Basato, M.; Biffis, A.; Martinati, G.; Tubaro, C.; Venzo, A.; Ganis, P.; Benetollo, F. *Inorg. Chim. Acta* **2003**, *355*, 399−403.
(27) Kee, H. L.; Bhaumik, J.; Diers, J. R.; Mroz, P.; Hamblin, M. R.; Bocian, D. F.; Lindsey, J. S.; Holten, D. *J. Photochem. Photobiol., A* **2008**, *200*, 346−355.
(28) Wasielewski, M. R.; Niemczyk, M. P. *J. Am. Chem. Soc.* **1984**, *106*, 5043−5045.
(29) Strachan, J.-P.; Gentemann, S.; Seth, J.; Kalsbeck, W. A.; Lindsey, J. S.; Holten, D.; Bocian, D. F. *J. Am. Chem. Soc.* **1997**, *119*, 11191−11201.
(30) Casper, J. V.; Meyer, T. J. *J. Phys. Chem.* **1983**, *87*, 952−957.
(31) Wilson, J. S.; Chawdhury, N.; Al-Mandhary, M. R. A.; Younus, M.; Khan, M. S.; Raithby, P. R.; Kohler, A.; Friend, R. H. *J. Am. Chem. Soc.* **2001**, *123*, 9412−9417.
(32) Whittle, C. E.; Weinstein, J. A.; George, M. W.; Schanze, K. S. *Inorg. Chem.* **2001**, *40*, 4053−4062.
(33) Barker, C. A.; Zeng, X.; Bettington, S.; Batsanov, A. S.; Bryce, M. R.; Beeby, A. *Chem.—Eur. J.* **2007**, *13*, 6710−6717.
(34) Ikai, M.; Ishikawa, F.; Aratani, N.; Osuka, A.; Kawabata, S.; Kajioka, T.; Takeuchi, H.; Fujikawa, H.; Taga, Y. *Adv. Funct. Mater.* **2006**, *16*, 515−519.
(35) Kwong, R. C.; Sibley, S.; Dubovoy, T.; Baldo, M.; Forrest, S. R.; Thompson, M. E. *Chem. Mater.* **1999**, *11*, 3709−3713.
(36) Crosby, G. A.; Demas, J. N. *J. Phys. Chem.* **1971**, *75*, 991−1024.
(37) Wang, Y.; Schanze, K. *Chem. Phys.* **1993**, *176*, 305−319.
(38) The views and conclusions contained in this document are those of the authors and should not be interpreted as representing the official policies, either expressed or implied, of the Defense Advanced Research Projects Agency; the U.S. Army Aviation and Missile Research, Development, and Engineering Center; or the U.S. Government.